



Polarization as a Tool in Calorimetry

N. Akchurin¹

Texas Tech University, Department of Physics, Lubbock, USA

Abstract

The signals from a high-Z scintillating crystal (BSO) are studied to characterize Cherenkov light polarization and to measure the longitudinal polarization profile of Cherenkov light in electromagnetic showers. The scintillation and Cherenkov lights can be separated by making use of the fact that the latter is polarized in the context of dual-readout calorimetry. In addition, this unique characteristic of Cherenkov light opens up a new set of possibilities that range from high-energy calorimetry to atmospheric air showers.

Keywords:

Polarization, Cherenkov, Calorimetry, Air showers

1. Introduction

Cherenkov light is distinguishable from other types of light by its unique and unusual features. Cherenkov photons are emitted at an angle θ_{ch} with respect to the direction of the charged particle whose energy is above a threshold, > 73 keV for electrons in BSO, for example. The Cherenkov spectrum is continuous and strongly peaked in the shorter ($1/\lambda^2$) wavelengths. It is also prompt compared to atomic or molecular transitions that emit photons. The characteristic that we focus on in this paper is its polarization: the electric field is perpendicular to the surface of the Cherenkov cone, whereas the magnetic field is tangent to it [1].

Two major measurements are reported in this paper. The first is the measurement of the Cherenkov light polarization in Section 2, and the second is the measurement of degree of polarization along the electromagnetic shower axis in Section 3. Some of the earlier results in the context of dual-readout calorimetry can be found in [2]. Possible applications and uses of this effect are discussed in Section 4.

2. Measurement of Polarization of Cherenkov Light

The fundamental element in all the measurements reported here is a block of ortho-bismuth silicate or BSO ($\text{B}_4\text{S}_3\text{O}_{12}$) crystal. It measures 18 cm in length and 2.2×2.2 cm² in cross section. Ten-stage, super-bialkali photocathode with borosilicate window Hamamatsu PMTs (H8900) are mounted on either end of the block (Figure 1). The Cherenkov side is equipped with a U330 filter that transmits lower wavelengths ($\lesssim 400$ nm), whereas the scintillation side with a GG495 filter transmits higher wavelengths ($\gtrsim 500$ nm). In addition to these filters, the polarizer sheets, HN38, can be inserted in any desired orientation, as indicated in Figure 1. To the extent possible, the refractive index

¹DREAM Collaboration: Texas Tech University, University and INFN-Pisa, INFN-Cagliari, University "La Sapienza" and INFN-Roma I, Iowa State University, University and INFN-Pavia, University of Calabria and INFN-Cosenza.

matching between the BSO and the PMT window is accomplished by silicone sheets². Three such sheets sandwich the filters between the BSO block and the PMTs on either side. Figure 1 displays the properties of these filters as well as the quantum efficiency (QE) for the H8900 PMT and the optical transmission characteristics of the BSO block [3]. The entire system is mounted on a remotely controlled rotation stage in the beam line, and the geometrical center of the block coincides with the rotation axis. The PMT signals are digitized using a 2.5 GHz Domino Ring Sampler (DRS) system within a 210 ns window. The first 20 ns of the pulse provides a baseline (pedestal) and the pulse shape is integrated offline.

Although the polarization measurements discussed here could be performed with many other crystals, the BSO proved practical for our purposes. It is relatively dense (6.80 g/cm^3), with a large index of refraction ($n = 2.06$) that gives a large Cherenkov angle ($\theta_{\text{ch}} = 61^\circ$). The radiation length is short ($X_0 = 11.5 \text{ mm}$), and the primary decay time is relatively short ($\sim 100 \text{ ns}$) at the peak emission (480 nm).

Three separate setups are developed to measure the polarization of Cherenkov light when the BSO block is impacted by high energy particles. Table 1 displays the orientation of the polarizers for each of these three cases. We used $180 \text{ GeV}/c \pi^-$ s and μ^- s at the H8 beam line at CERN for these measurements. The *favorable* orientation refers to the polarizer orientation where horizontal components of the electric field are transmitted, as shown in Figure 2.c. The *unfavorable* orientation refers to the situation depicted in Figure 2.d where the vertical components of the electric field on average add to zero; thus little or no Cherenkov light is transmitted.

Table 1: The orientation of polarizers for three different setups the Cherenkov light polarization measurement discussed in Section 2.

Setup No	Cherenkov Side	Scintillation Side
0	No Polarizer	No Polarizer
1	Favorable	Favorable
2	Unfavorable	Favorable

Respectively, Figures 3.a and 3.c show the scintillation and Cherenkov signals as a function of the rotation angle, θ . In this setup (Setup 0), no polarizers are used to establish a baseline. Both signals are normalized such that at $\theta = 0^\circ$ they equal unity. The small black squares are calculated and equal $1/\cos\theta$ in order to represent the increase in a charged particle's path length in the BSO block. The open circles represent signals generated by muons, whereas the solid squares are for pions. We elected to treat muons and pions separately so as to be sensitive to the interaction effects as θ increased. The scintillation signal is divided by $\cos\theta$ (Figure 3.b), and we observe that there is neither significant hadronic interaction nor unisotropy in the way that scintillation light is produced in the BSO block. The Cherenkov light clearly peaks at $\theta = -29^\circ$, which corresponds to the Cherenkov angle $\theta_{\text{ch}} = 61^\circ$ (see Figure 1) as depicted in Figure 3.d.

Figure 4 displays the measurements with polarizers installed in favorable orientation at both ends of the BSO block (Setup 1). The scintillation light is isotropic and unpolarized, as indicated by Figure 4.a; however, a small amount of polarized Cherenkov light peaking at $\theta = +29^\circ$ is detected by the scintillation PMT. This is better represented in Figure 4.b, where the scintillation signal is divided by $\cos\theta$ to remove the effect of varying path length with changing θ . Otherwise, the favorable orientation of the polarizers in this case does not significantly alter the picture compared to the no-polarizer arrangement that is already discussed above (Setup 0). We note that in both Figure 3.c and Figure 4.c some Cherenkov light is reflected back to the Cherenkov PMT at $\theta = +29^\circ$. Typically 12% of the normally incident light inside the BSO block is reflected back by the end surface.

The unfavorable orientation of the polarizer at the Cherenkov end drastically changes the situation (Setup 2). Figures 5.c and 5.d reveal that the unfavorable orientation of the polarizer causes suppression of the Cherenkov signal, largest at the Cherenkov angle ($\theta = -29^\circ$). The horizontal polarization components of the Cherenkov light are essentially blocked by the polarizer. As expected, there is no change in the scintillation signal between Setup 1 and Setup 2.

²Elastosil RT 601 with the refractive index $n = 1.4095$ with $\geq 88\%$ in the wavelengths of interest.

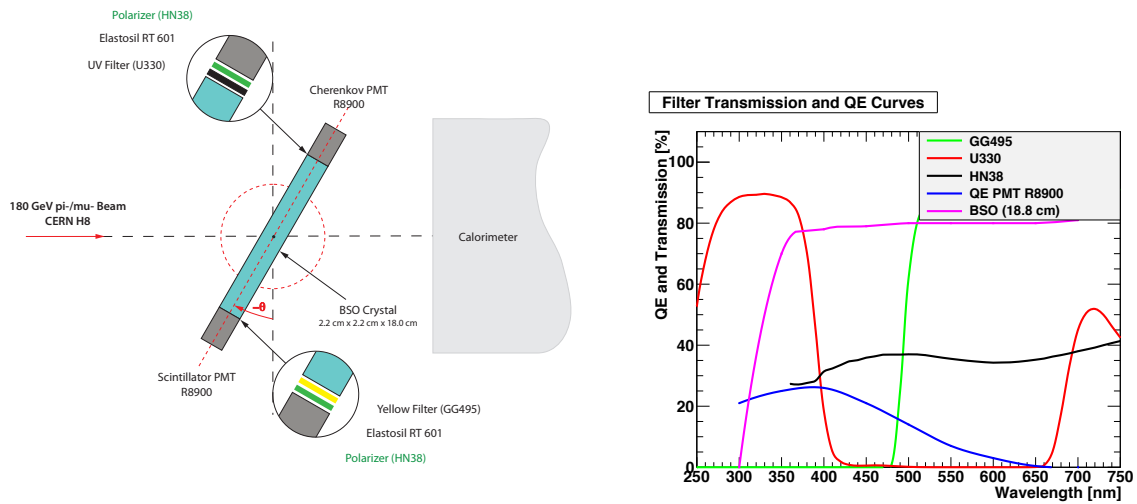


Figure 1: The experimental setup includes a BSO crystal equipped with two PMTs mounted on a rotation stage. The rotation angle θ is zero when the block is perpendicular to the beam direction. Note that the Cherenkov light is most efficiently directed towards the Cherenkov PMT at $\theta = -29^\circ$ or at the Cherenkov angle ($\theta_{ch} = 61^\circ$). A hadronic calorimeter on the right helps identify muons and pions (left). The spectral transmission properties of the filters are displayed on the right. We detect mostly Cherenkov light on one end of the block where the U330 filter is installed. Mostly scintillation light is detected at the longer wavelengths with the use of the GG495 filter on the other end of the block. The polarizer HN38 is effective at all relevant wavelengths with $\gtrsim 30\%$ transmission.

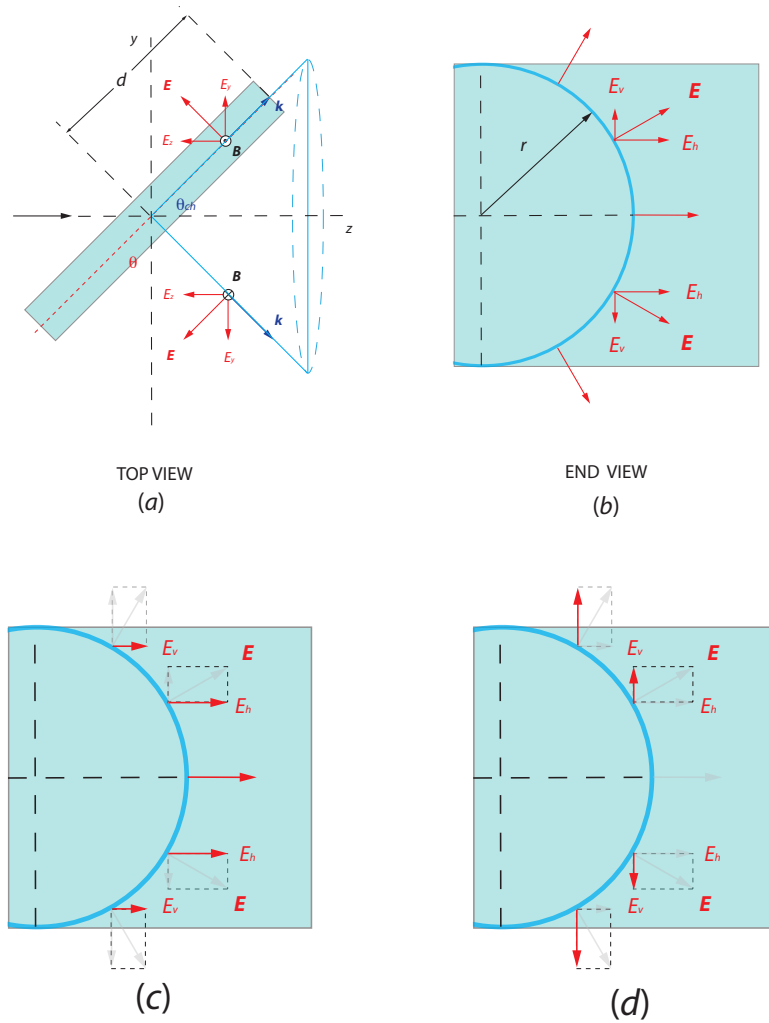


Figure 2: When viewed from the top (a), a cone section (Cherenkov cone) is developed in the BSO block as a charged particle traverses the block as indicated by a black arrow. The end view (b), as seen by the Cherenkov PMT, sees an arc or a piece of the Cherenkov cone. The polarization directions are shown on this exaggerated projection of the cone onto the block end. In our setup, the radius of the cone at the Cherenkov PMT is about 7.8 cm. The favorable direction is defined when the horizontal components of the electric field vectors E_h are parallel and transmitted through the polarizer (c). The polarizer is in an unfavorable direction when it is oriented such that the vertical components of the electric field vectors E_v are transmitted and tend to add to zero (d).

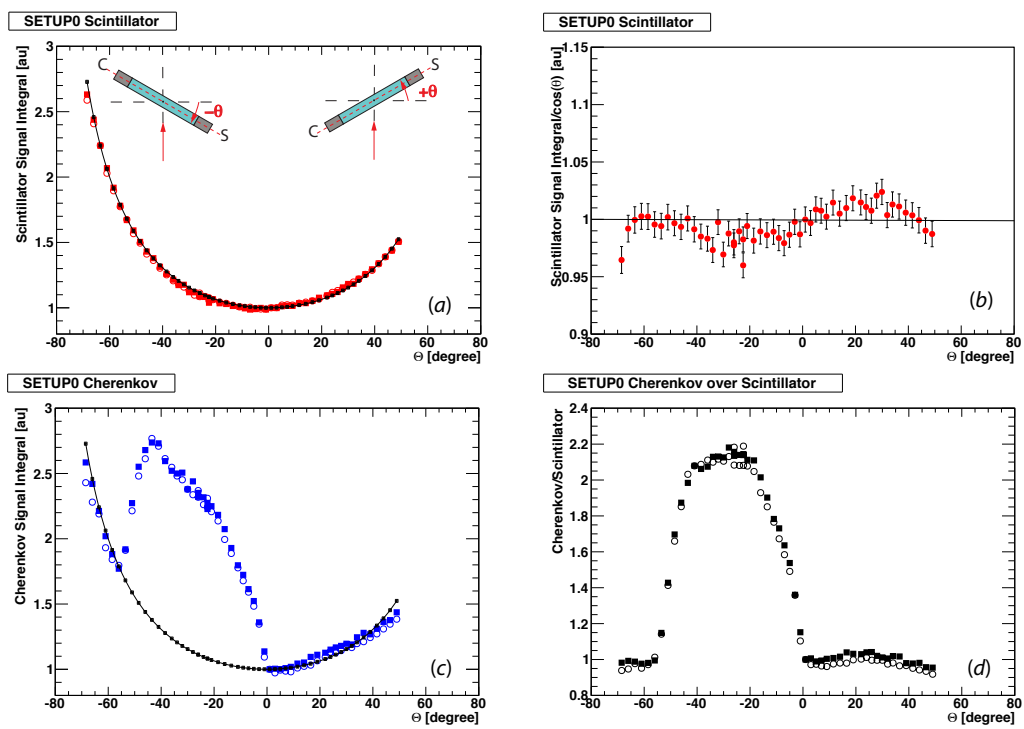


Figure 3: The scintillation (a) and Cherenkov (c) signals are measured as a function of the angle of incidence θ for Setup 0 (see Table 1). The scintillation signal is divided by $\cos \theta$ in (b) and C/S in (d). See text for discussion.

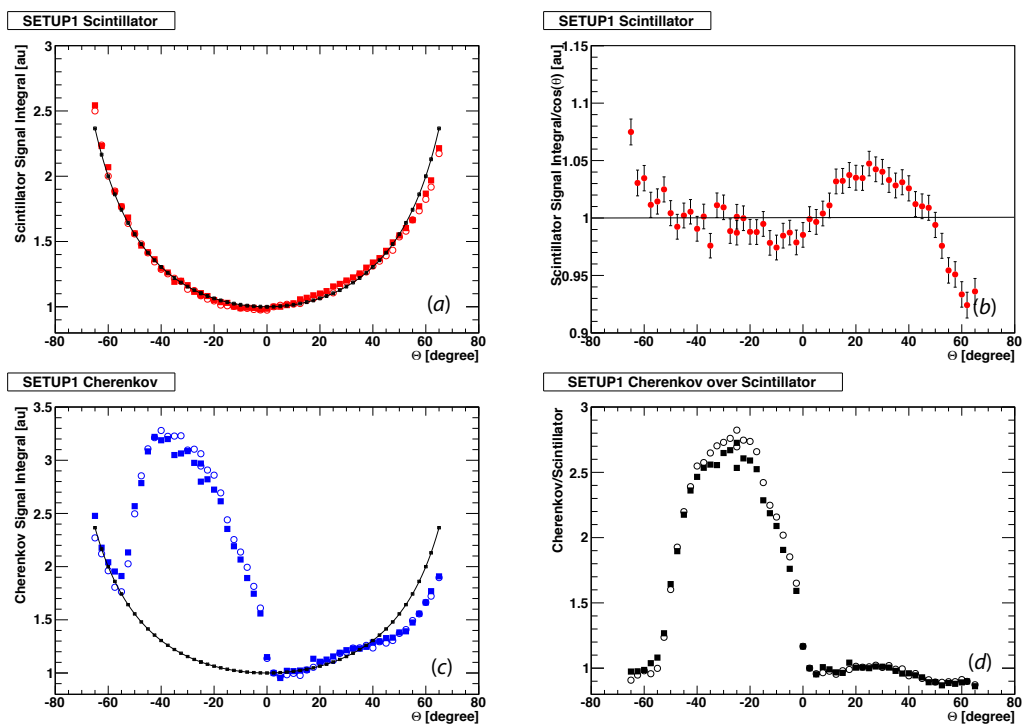


Figure 4: The scintillation (a) and Cherenkov (c) signals are measured as a function of the angle of incidence θ for Setup 1 (see Table 1). The scintillation signal is divided by $\cos \theta$ in (b) and C/S in (d). See text for discussion.

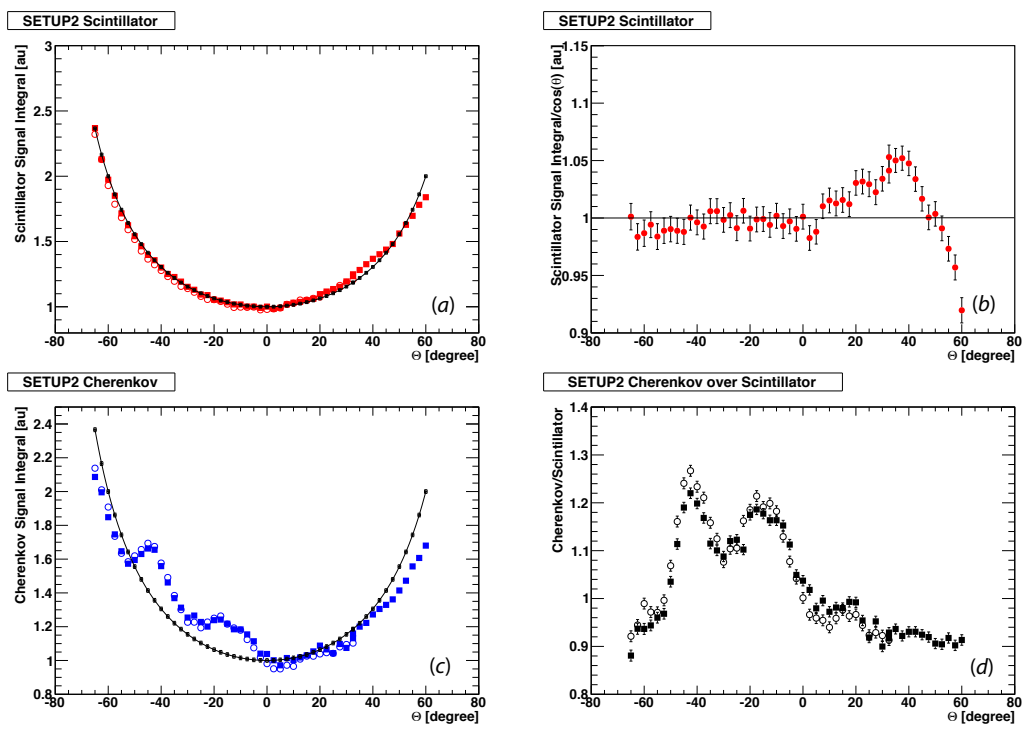


Figure 5: The scintillation (a) and Cherenkov (c) signals are measured as a function of the angle of incidence θ for Setup 2 (see Table 1). The scintillation signal is divided by $\cos \theta$ in (b) and C/S in (d). See text for discussion.

3. Measurement of Cherenkov Light Polarization in EM Showers

An interesting question is if and to what extent Cherenkov polarization is maintained in the development of showers. For investigation of the degree of polarization as a function of longitudinal depth, lead sheets are stacked upstream of the BSO block as depicted in Figure 6. The BSO block is positioned at $\theta = -30^\circ$ such that the Cherenkov light is directed towards the Cherenkov PMT for a through-going particle. The longitudinal shower profiles using an 80 GeV/c electron beam are measured with favorable and unfavorable polarizer orientations. Figure 7 shows these normalized profiles such that at the shower maximum, the signals are set to unity. As the shower develops in the calorimeter, the direction of the secondary particles increasingly become random. Before the shower maximum, the number of secondary shower particles is small and their directions are strongly aligned with that of the incoming particle's direction. Therefore, the Cherenkov polarization direction tends to be maintained as Figure 7 shows. Once the shower has fully developed, there is no longer a preferred momentum direction among the shower particles, and the polarization averages to zero. A simple em longitudinal shower profile parametrization, $\frac{dE}{dt} = Ct^a e^{-bt} + \delta$, helps in quantifying these phenomena for favorable (Figure 7.a) and unfavorable (Figure 7.b) polarizer orientations. It should be noted that in the case of favorable polarizer orientation, the Cherenkov signal appears earlier in depth compared to the scintillation light. In the case of the unfavorable polarizer orientation, there is no difference between the Cherenkov and scintillation light profiles because the Cherenkov polarization is suppressed by the polarizer and only randomly polarized Cherenkov light results in measurable signal. The a parameter obviously shows this difference when the data points are fitted with the above parametrization (Table 2). Figures 7.c and 7.d further illustrate the same where the Cherenkov (C) signal at a given depth is divided by the scintillation (S) signal. In the favorable case (Figure 7.c), the $C/S > 1$ for $t \lesssim t_{\max}$, whereas $C/S \sim 1$ for all t in the unfavorable case (Figure 7.d). The exponential tail of dE/dt is quantified by b , and there is no significant difference between the favorable, unfavorable, and/or scintillation cases. The superimposed curves in Figures 7.c and 7.d are the ratios of the fitted curves for the dE/dt profiles in Figures 7.a and 7.b and are not fits to C/S data.

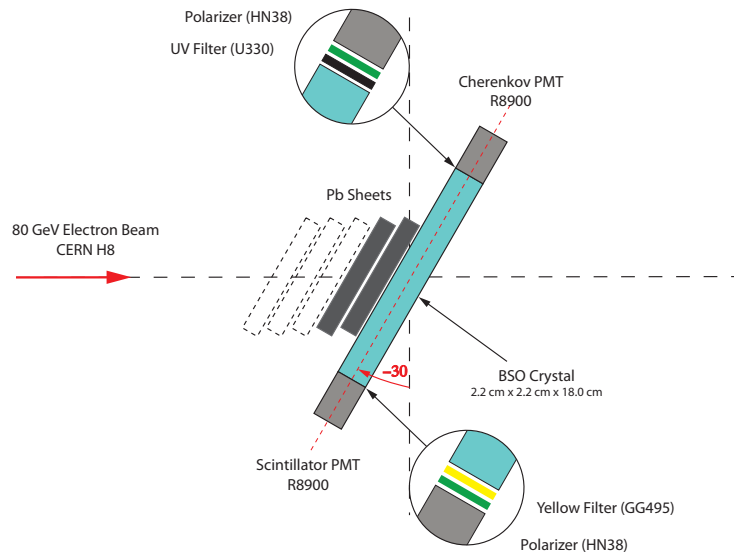


Figure 6: The setup used for the longitudinal Cherenkov light polarization measurement where the polarizer at the Cherenkov end is oriented in favorable and unfavorable orientations.

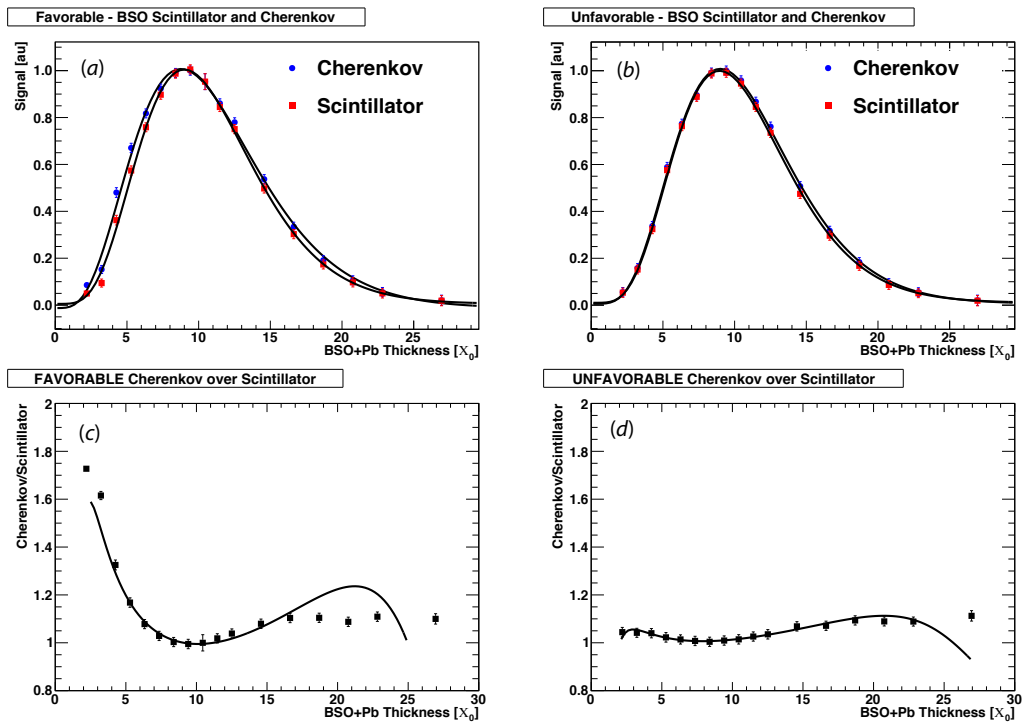


Figure 7: The longitudinal shower profile measurements using 80 GeV/c electrons are measured using favorable (a) and unfavorable (b) polarizer orientations at the Cherenkov end. The bottom two plots show the C/S ratios for these two cases where the enhanced Cherenkov signal is clearly visible in (c). The curves in the bottom two plots are the ratio of fitted curves above and not fits to C/S data itself.

Table 2: The fit results for the a and b parameters are given for the two cases: the favorable (Figures 7.a and 7.c) and the unfavorable orientation of the polarizer at the Cherenkov end (Figures 7.b and 7.d). The orientation of the polarizer at the scintillation end is the same in both cases and is not relevant.

Setup	Signal	a	b
Favorable	Scintillation	5.11 ± 0.28	0.568 ± 0.029
	Cherenkov	4.08 ± 0.25	0.465 ± 0.028
Unfavorable	Scintillation	5.18 ± 0.28	0.579 ± 0.030
	Cherenkov	4.94 ± 0.27	0.549 ± 0.029

4. Remarks and Conclusions

Cherenkov light polarization adds another unique and discriminating feature still to be exploited in the field of calorimetry. It may be possible to improve energy and direction measurements of high energy particles as we further explore Cherenkov radiation. Although the timing and the spectral characteristics of the Cherenkov light lend themselves to easier utilization for discrimination against scintillation light in the context of dual-readout calorimetry, the full potential of the polarization has yet to be fully determined. The data presented here show that the polarization of Cherenkov light is clearly measurable and that in the early part of showers, the polarization remains intact. These features may become useful, for example, in the study of air showers as the Cherenkov ring on the earth surface will maintain the polarization directions, as sketched in Figure 8. The Cherenkov photons from the earlier part of the shower will map onto the outer circle with clear polarization direction, while the Cherenkov photons from the later part of the shower will map onto the inner part of the light pancake and will have zero net polarization because the directions of charged particles within the shower will largely be random. Therefore, use of polarizers with known orientations on the surface detectors will allow to better detail the early shower development in the upper atmosphere and may also allow hadron vs electromagnetic interaction discrimination.

The concurrent detection of Cherenkov and scintillation signals is the principal concept of dual-readout calorimetry because the ratio of Cherenkov to scintillation signal is a measure of the em fraction in a hadronic shower on an event-by-event basis. Therefore, the fluctuations in the em fraction can be measured and eliminated, improving performance. The degree to which the Cherenkov polarization is a discriminant in this context remains to be fully explored. Polarization of Cherenkov radiation in itself may also prove helpful, as indicated above in the case of air showers. It may also be possible to further investigate the em core of hadronic showers through the polarization information to further control dominating fluctuations that degrade performance. Some ideas are now being tested via simulations.

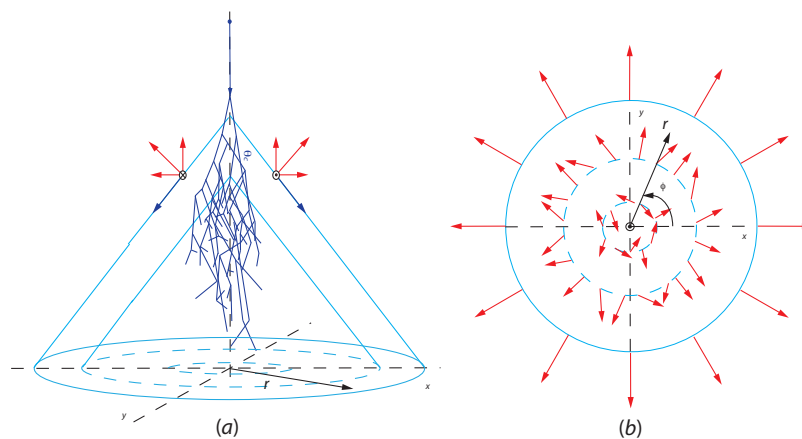


Figure 8: Air showers are typically initiated by single high energy particles 10-20 km above earth (a). The size of the light pancake on the earth surface measures $r \sim 100$ to 200 m. The electric field vectors are indicated in red. The Cherenkov polarization direction is expected to be better preserved at larger r values (b).

- [1] P. A. Cherenkov, *Compt. Rend.* **2** (1934) 451 and I. Frank and I. E. Tamm, *Dokl. Akad. Nauk SSSR* **14** (1937) 109.
- [2] N. Akchurin *et al*, *Nucl. Instr. Meth. A* 638 (2011) 47-54.
- [3] H. Shimizu *et al*, *Nucl. Instr. Meth. A* 550 (2005) 258-266.